REVIEW ARTICLE

The anomalous skin effect in gas discharge plasmas

V I Kolobov and D J Economou

Plasma Processing Laboratory, Department of Chemical Engineering,
University of Houston, Houston, TX 77204-4792, USA

Abstract. This paper contains a review of classical and recent works on the anomalous skin effect in gas discharge plasmas. Recently, interest in this problem has been generated by the introduction of inductively coupled plasma (ICP) sources operating at low gas pressures (0.1–50 mTorr). The near-collisionless operating regime corresponds to the conditions of the anomalous skin effect. The skin effect governs not only the distribution of the electromagnetic field but also the mechanism of electron heating and power absorption by the plasma. The finite dimensions of the plasma and magnetic fields as weak as the natural geomagnetic field play important roles under these conditions. The understanding of these phenomena is far from complete. We draw upon advances in the physics of metals (where the anomalous skin effect was discovered and thoroughly explored) to gain insight into discharge plasmas where many interesting phenomena are yet to be found.

1. Introduction

It is known that an alternating electromagnetic field is damped within a conductor, and not only the field but also the resulting electric current is concentrated near the surface of the conductor. This is called the skin effect. We shall consider the case when the field frequency ω is less than the electron plasma frequency ω_p. In simple cases, the nature of the skin effect is determined by the relative magnitude of three characteristic lengths: the skin depth δ, the electron mean free path λ, and the length v/ω which an electron traverses during the field period (v is a characteristic electron velocity) [1]. Although the skin effect depends to some extent on characteristics of the conductor (such as the electron distribution function), there are many features common to all conductors. We shall compare phenomena in gas discharges with those in metals where the anomalous skin effect was discovered experimentally by London [2] in 1940 and thoroughly explored afterwards. Nowadays, considerable interest in this problem exists due to extensive studies of low-pressure inductively coupled plasmas (ICPs) where the anomalous skin effect plays an important role.

ICPs are weakly ionized plasmas with plasma density $n \approx 10^{10}$–10^{12} cm^{-3}, electron collision frequency with neutrals $v \approx 10^7$ s^{-1} (at argon gas pressure 5 mTorr), and a near-Maxwellian electron energy distribution with temperature $T_e \approx 5$ eV [3]. For a typical driving frequency $\omega = 8.5 \times 10^7$ s^{-1} (13.56 MHz) the inequality $\omega < \omega_p$ holds true for plasma density $n_c > 2 \times 10^6$ cm^{-3}. The electron mean free path λ becomes comparable to the characteristic

size of plasma devices $L \approx 10$ cm at pressures of about 3 mTorr. The finite dimensions of the plasma must be important for electron kinetics and the skin effect under these conditions. In addition, magnetic fields as weak as the natural geomagnetic field (≈ 0.5 G) may affect such a plasma because the electron Larmor radius r_H becomes comparable to λ at $B \approx 1$ G.

The electron gas in metals obeys Fermi statistics [4]. For ordinary metals, in which the number of conducting electrons is of the order of one electron per atom, $\omega_p \approx 10^{15}$–10^{16} s^{-1}. At the frequencies usually employed in radio engineering (up to $\omega = 10^{10}$ s^{-1}), the condition $\omega \ll \omega_p$ is satisfied within a large margin. In metals, δ is usually small compared to λ (see table 1)†. Plasma parameters in metals and in ICPs are compared in table I. Moreover, the effective boundary of a discharge plasma is not abrupt as in metals, but is formed by the shape of the electrostatic potential in the discharge. While electrons reflect specularly by the potential barrier at the wall, reflections from the metal boundaries are to some extend diffuse.

The theory of the skin effect in metals has been well developed. Several new physical phenomena have been reported for thin metal films. In particular, application of static magnetic fields to the films has resulted in a variety of finite-size and resonance effects [4]. In

---

† The calculation of λ is one of the basic problems in the theory of metals. One should consider electron collisions with (a) phonons (lattice vibrations), (b) other electrons, and (c) impurity atoms and defects of the lattice.

Table 1. Plasma parameters in metals and in inductively coupled gas discharges.

	n_e (cm^{-3})	λ (cm)	ω_p (s^{-1})	v (cm s^{-1})	δ (cm)
Metal	10^{22}	0.1	10^{15}	10^{8}	10^{-5}
ICP	10^{11}	10	10^{10}	10^{8}	1

contrast, the skin effect in discharge plasmas is relatively unexplored. In some respects, gas discharges are better suited for basic studies of this effect compared to metals; for instance, precise measurements of spatial distributions of the electromagnetic fields can be performed in gaseous plasmas by using magnetic probes. Recent interest in ICPs generated by the development of new plasma technologies has prompted further studies of the anomalous skin effect— the mechanisms of electron heating and power absorption in ICPs are closely related to the skin effect. This is another subject where basic plasma research meets the world of semiconductor manufacturing.

In what follows, we shall briefly describe classical and recent works on the anomalous skin effect. We will draw upon the advances made in the physics of metals to gain insight into what one might expect to find in discharge plasmas. This paper is an extention of a memorandum compiled at the Plasma Processing Laboratory at the University of Houston in June 1996 [5].

2. Electrodynamics of good conductors

The principal characteristic of a good conductor is the high density of conducting electrons. In such a conductor, the displacement current generated by the time varying electromagnetic fields is small compared to the conduction current, and the Maxwell equation (in a Gaussian system)

$$\nabla \times \boldsymbol{H} = \frac{4\pi}{c}\boldsymbol{j} + \frac{1}{c}\frac{\partial \boldsymbol{D}}{\partial t} \qquad (1)$$

is reduced to the quasi-static equation

$$\nabla \times \boldsymbol{H} = \frac{4\pi}{c}\boldsymbol{j}. \qquad (2)$$

Ampere's law (2) defines the magnetic field which is generated by external sources and by currents in the plasma in the limit $\omega \ll \omega_p$. It follows from (2) that $\nabla \cdot \boldsymbol{j} = 0$, i.e. the use of (2) corresponds to neglecting the time variation of the space charge in the conductor. Faraday's law

$$\nabla \times \boldsymbol{E} = -\frac{1}{c}\frac{\partial \boldsymbol{B}}{\partial t} \qquad (3)$$

defines a solenoidal electric field which is induced by the time-varying magnetic field. The difference between $\boldsymbol{B}$ and $\boldsymbol{H}$ is unimportant for the nonferromagnetic materials we consider. The determination of the field structure in the conductor requires self-consistent solution of (2) and (3) with the current density $\boldsymbol{j}$ in the 'plasma' as a function of the (yet to be found) fields.

In calculating the current density, $\boldsymbol{j}$, we can have two limiting cases. If the characteristic length δ (skin depth) in which the field changes significantly is large compared to the characteristic scale l describing the electron motion (the shortest of λ, r_H, and v/ω), the relationship between $\boldsymbol{j}$ and $\boldsymbol{E}$ is *local*

$$\boldsymbol{j} = \hat{\sigma} \boldsymbol{E} \qquad (4)$$

where $\hat{\sigma}$ is the conductivity tensor. The skin effect is said to be normal when Ohm's law (4) holds true and there is no temporal dispersion of σ.

Another limiting case corresponds to the extreme anomalous skin effect when δ is small: $\delta \ll l$. In this case, the current density at a given point is a function of the fields along the entire electron trajectories (*non-local* case). However, only a small number of electrons make a considerable contribution to the current density. These are 'glancing' electrons which are reflected at small angles ($\sim\delta/\lambda$) from the plasma boundary and thus spend a considerable part of the field period within the skin layer. The rest of the electrons escape the skin layer too rapidly to make a considerable contribution to the current. The separation of the electrons into two groups is useful in the development of a qualitative theory of the anomalous skin effect.

The phenomena which constitute the essence of the anomalous skin effect were first noticed by London in 1940. The qualitative theory of the effect is due to Pippard [6], and the quantitative theory is due to Reuter and Sondheimer [7] who considered the simple case of a semi-infinite metal with no static magnetic field. Since that time, the anomalous skin effect in metals has been thoroughly studied [4, 8].

Demirkhanov *et al* [9] were the first to experimentally observe anomalies of the skin effect in a gas discharge plasma. Their results stimulated many theoretical and experimental works devoted to this effect [10–20]. Nonmonotonic profiles of the rf fields, finite-size effects, and resonance phenomena were experimentally found and explained in inductive discharges. The works [21–23] were triggered by studies of microwave pinch discharges. These theoretical works focused on the effects of the non-sharpness of plasma boundaries and the role of static magnetic fields. Recent interest in the field has been generated by the application of low-pressure ICP sources for materials processing. The near-collisionless operating regime and the geometry of modern ICP sources are historically unusual and have not been extensively studied until recently. The anomalous skin effect is important for ICP operation in this regime. While ICPs have become widely used in practice, some basic questions about their operation remain poorly understood. Among these questions are the mechanism of electron heating, the role of magnetic fields on electron kinetics, and the peculiarities of the skin effect in a bounded plasma.

3. Skin effect in a semi-infinite plasma in the absence of a static magnetic field

Let us consider the simple case of an electromagnetic wave incident on a semi-infinite spatially uniform plasma with

no static magnetic field. For any angle of incidence of the wave, the problem becomes one dimensional and all quantities depend only on the distance x from the surface. The nature of the wave reflection from and absorption by the plasma defines the tangential components of the electric field $\boldsymbol{E}_t^s$ and the magnetic field $\boldsymbol{H}_t^s$ at the plasma surface

$$\boldsymbol{E}_t^s = \hat{\zeta}[\boldsymbol{H} \times \boldsymbol{n}]_t^s. \qquad (5)$$

Here $\boldsymbol{n}$ is a unit vector normal to the surface and the quantity $\hat{\zeta} = \hat{\zeta}' + \mathrm{i}\hat{\zeta}''$ is called the surface impedance† (which is a two-dimensional tensor in electrically anisotropic media [4]). The real and imaginary parts of $\hat{\zeta}$ determine the energy dissipated in the plasma and the phase shift of the field resulting from the wave reflection by the plasma, respectively. The calculation of $\hat{\zeta}$ requires knowledge of the current density $\boldsymbol{j}$ induced in the plasma by the electromagnetic fields of the wave.

3.1. Classical skin effect

When the thermal motion of electrons is neglected (cold plasma), the relation between the current density $\boldsymbol{j}$ and the field $\boldsymbol{E}$ is given by Ohm's law (4). Consider the simplest case of an isotropic medium where σ is a scalar. According to (2)–(4), the damping of the electric field of a monochromatic wave (all quantities varying as $\propto \exp(\mathrm{i}\omega t)$) in such a medium is described by the complex equation

$$\frac{\mathrm{d}^2 E}{\mathrm{d}x^2} = \frac{4\pi \mathrm{i}\omega\sigma}{c^2} E. \qquad (6)$$

In the general case σ is a complex quantity accounting for electron inertia. For real σ the amplitude of the electric field decreases exponentially from the surface [24]

$$E = E_0 \, \mathrm{e}^{-x/\delta} \cos(x/\delta - \omega t) \qquad (7)$$

with the skin depth δ given by

$$\delta^{-1} = \mathrm{Re}\left(\frac{4\pi \mathrm{i}\omega\sigma}{c^2}\right)^{1/2} \qquad (8)$$

and the phase of the field is a linear function of the coordinate x. In this case, $\boldsymbol{E}_t = \zeta[\boldsymbol{H} \times \boldsymbol{n}]_t$ not only on the surface but throughout the entire half-space, and the scalar plasma impedance is given by

$$\zeta = (1 + \mathrm{i})\sqrt{(\omega/8\pi\sigma)}. \qquad (9)$$

The inequality $\zeta' > 0$ ensures energy dissipation and must always be satisfied.

If the collision frequency ν is independent of electron energy, the conductivity σ is given by [25]

$$\sigma = \frac{n_e e^2}{m(\nu + \mathrm{i}\omega)} \qquad (10)$$

where e is the electron charge, m is the electron mass, and n_e is the electron density. Substituting (10) into (8) one obtains the classical skin depth [10]

$$\delta = \delta_0 / \cos(\epsilon/2) \qquad (11)$$

† This name is also given to the quantity $\mathcal{Z} = 4\pi\zeta/c$.
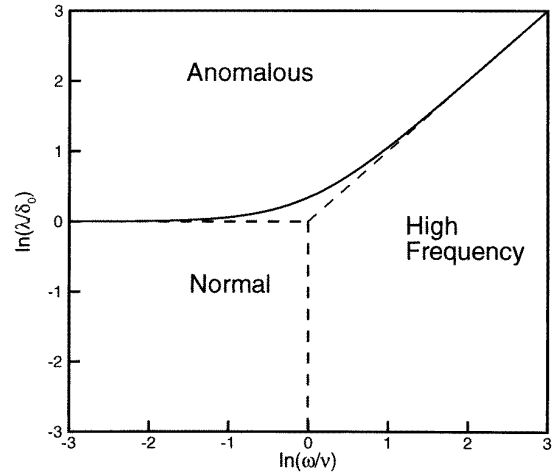
Figure 1. Skin effect in a semi-infinite plasma with no magnetic field. δ_0 is defined by equation (12). The solid line, corresponding to $\Lambda = 1$, is the boundary of the anomalous skin effect.

where

$$\delta_0 = \frac{c}{\omega_p}\left(1 + \frac{\nu^2}{\omega^2}\right)^{1/4} \qquad \epsilon = \tan^{-1}(\nu/\omega). \qquad (12)$$

At low frequencies, $\omega \ll \nu$, the skin depth is $\delta_n = (c/\omega_p)\sqrt{2\nu/\omega}$ and the energy dissipation is due to collisions. This is the normal skin effect (see figure 1). At high frequencies, $\omega_p \gg \omega \gg \nu$, (the high-frequency region in figure 1), the (collisionless) skin depth is $\delta_p = c/\omega_p$ and the impedance $\zeta = \mathrm{i}\omega\delta_p/c$ is purely imaginary. The wave is reflected from the plasma without energy dissipation. In metals, the high-frequency region corresponds to the infrared range of wavelengths [4].

If ν is a function of electron energy, ε, equation (10) is replaced by the more general form [26]

$$\sigma = \frac{n_e e^2}{m(\nu_{eff} + \mathrm{i}\omega_{eff})} \qquad (13)$$

where the effective frequencies ν_{eff} and ω_{eff} depend on both $\nu(\varepsilon)$ and ω. Using (13) allows one to obtain the thickness of the skin layer and the plasma impedance in terms of ν_{eff} and ω_{eff}.

3.2. Anomalous skin effect

When electrons move a distance comparable to the skin depth during the field period, and do not collide in that time, the conductivity becomes a function of the rf field throughout the entire skin layer [6, 7]. The skin effect under these conditions is said to be anomalous (see figure 1). In the extreme anomalous case (a) neither the skin depth δ nor the surface impedance ζ depend on the collision frequency ν, (b) the dissipation of energy is present even if $\nu = 0$, (c) the damping of the field is characterized by at least two characteristic lengths, and (d) the field profile can be non-monotonic, and in some places the current can even flow against the field.

The qualitative theory of the anomalous skin effect is due to Pippard [6]. Pippard suggested that the main contribution to the skin current is made by 'effective' electrons moving almost parallel to the surface. The velocity of these electrons forms angles less than δ/λ with the surface. The relative number of 'effective' electrons is of the order of δ/λ. The remaining 'ineffective' electrons leave the skin layer too quickly and therefore the electric field has little time to affect them. The concept of separating electrons into two groups has proven to be useful in the theory of the anomalous skin effect.

For a qualitative treatment, one can introduce the effective conductivity of the skin layer

$$\sigma_{eff} = (\delta/\lambda)\kappa\sigma \tag{14}$$

where σ is the static conductivity ($\omega \ll \nu$) and the numerical constant $\kappa \approx 1$, and use Ohm's law (4). This way one obtains the anomalous skin depth

$$\delta_a = \left(\frac{c^2\lambda}{4\pi\omega\kappa\sigma}\right)^{1/3} \tag{15}$$

and the surface impedance

$$\zeta = \zeta' + i\zeta'' = \frac{1+i\sqrt{3}}{2}\left(\frac{\omega^2\lambda}{4\pi c\kappa\sigma}\right)^{1/3}. \tag{16}$$

A rigorous calculation confirms these formulae and yields $\kappa = \sqrt{\pi}$ for a Maxwellian plasma [10]. Equations (15) and (16) describe the principal features of the anomalous skin effect: (a) the independence of δ_a and ζ on the electron mean free path because $\sigma \sim \lambda$, (b) the dependence on frequency in the form $\zeta \sim \omega^{2/3}$ (in the normal skin effect this dependence is given by $\zeta \sim \omega^{1/2}$), and (c) the complex nature of ζ ($\zeta''/\zeta' = \sqrt{3}$), whereas in the normal skin effect $\zeta'' = \zeta'$.

A quantitative approach requires solution of the problem of propagation of a transverse electromagnetic wave, when the induced current at a given point is determined by the field distribution in the vicinity of the point within an electron free path. For the first time this problem was solved in [7] for a semi-infinite metal with Fermi distribution of electrons. Weibel [10] extended the theory to a gaseous plasma with a Maxwellian electron distribution function (EDF). For specular reflection of electrons at the plasma boundary, the problem is reduced to the solution of an integro-differential equation

$$\frac{d^2E}{dx^2} = \frac{i\omega\omega_p^2}{c^2}\int_{-\infty}^{\infty} K_v((i\omega+\nu)|x-x'|)E(x')\,dx' \tag{17}$$

where the kernel $K_v(\alpha)$ for a Maxwellian distribution is

$$K_v(\alpha) = \frac{1}{v\sqrt{\pi}}\int_0^{\infty}\frac{1}{\xi}\exp\left(-\alpha/v\xi - \xi^2\right)d\xi. \tag{18}$$

As the electron velocity v tends to zero (cold plasma), $K_v(\alpha)$ tends to a delta function, and equation (17) is reduced to equation (6) with σ given by (10). By a simple change of scale $z = |i\omega + \nu|x/v$, equation (17) can be cast in the form

$$\frac{d^2E}{dz^2} = i\Lambda\int_{-\infty}^{\infty} K(s|z-z'|)E(z')\,dz' \tag{19}$$
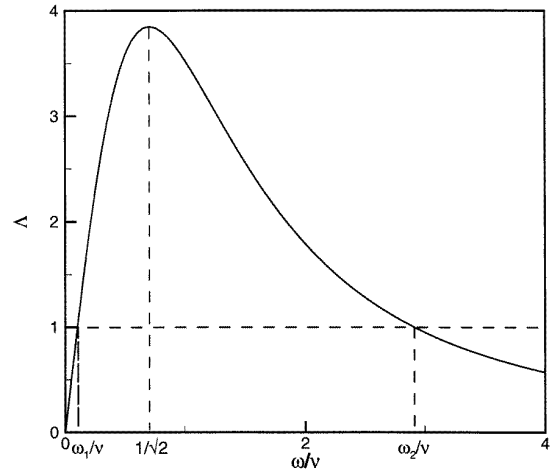
Figure 2. The parameter Λ as a function of ω/ν. The anomalous skin effect takes place in the frequency range $\omega_1 < \omega < \omega_2$.

where $K(\alpha)$ is the function $K_v(\alpha)$ for $v = 1$ and the parameters Λ and s are defined as

$$\Lambda = \left(\frac{\omega_p v_T}{c}\right)^2\frac{\omega}{(\omega^2+\nu^2)^{3/2}} \tag{20}$$

$s = i\exp(-i\epsilon)$ and ϵ is given by equation (12). The parameter Λ is a fundamental measure of non-locality of electromagnetic phenomena in plasmas [20]. Indeed, the ratio of the effective mean free path $\lambda_{eff} = v_T/\sqrt{\nu^2+\omega^2}$ to the classical (local) skin depth (11) is $\lambda_{eff}/\delta = \sqrt{\Lambda}$ (for $\omega \ll \omega_p$). The non-local effects are pronounced if λ_{eff} exceeds δ ($\Lambda > 1$), and they are small otherwise. It is significant that the parameter Λ becomes small both for low and high frequencies and has a maximum at $\omega \approx \nu$ (figure 2). It means that in both low- and high-frequency cases the penetration of electromagnetic waves into a plasma can be described as a classical skin effect.

The solution of equation (19) is found using Fourier transforms

$$E(z) = -\frac{E'(0)}{\pi}\int_{-\infty}^{\infty}\frac{e^{ikz}\,dk}{k^2 + i\Lambda h(k)}. \tag{21}$$

Here $h(k)$ is the Fourier transform of $K(z)$:

$$h(k) = \int_{-\infty}^{\infty} K(|z|)\,e^{-ikz}\,dz = \frac{1}{ik}Z(is/k). \tag{22}$$

$Z(\xi)$ is the plasma dispersion function (see for example [27]) and $E'(0)$ denotes dE/dz at $z = +0$. The solution $E(\Lambda, s, z)$ depends on the parameters Λ and s or ϵ (figure 3). Small values of Λ correspond to the normal case. Anomalies (e.g. non-monotonic field decay) begin to be noticeable for $\Lambda > 1$.

The surface impedance $\zeta = (i\omega/c)E(0)/(dE(0)/dx)$ is a measure of the wave reflection and absorption by the plasma. Using equation (21), one finds

$$\zeta = \frac{-i\omega\lambda_{eff}}{\pi c}\int_{-\infty}^{\infty}\frac{dk}{k^2 + i\Lambda h(k)}. \tag{23}$$
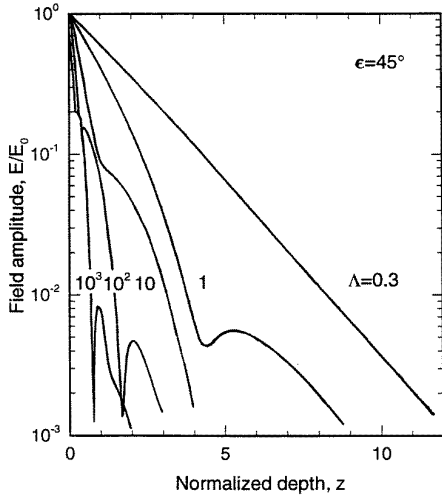
Figure 3. The amplitude of the electric field E as a function of normalized depth z for different Λ and $\nu/\omega = 1$ [10].
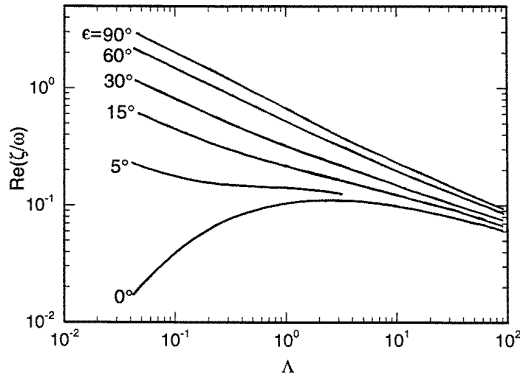
Figure 4. Real part of normalized surface impedance as a function of Λ and ϵ [10]. $\epsilon = 0$ corresponds to the collisionless case where $\Lambda = (v_T\omega_p/c\omega)^2$, and $\epsilon = \pi/2$ corresponds to collisional case where $\Lambda = (v_T\omega_p/cv)^2\omega/\nu$. The anomalous skin effect takes place at $\Lambda > 1$.

The real part of the surface impedance is shown in figure 4 as a function of Λ for different degrees of plasma collisionality ϵ. The real part of the surface impedance does not vanish at $\nu = 0$ (see figure 4; curve $\epsilon = 0$) and for the extreme anomalous case the dissipation of energy is independent of ν (lines in figure 4 'converge' for $\Lambda \gg 1$).

For $\Lambda > 1$ it is impossible to describe the field profile as a damped exponential wave (see figure 3). The field profile is affected by two components of the current. One is due to the 'effective' electrons which cause a sharp decrease of the field within the skin layer. The other is due to the 'ineffective' electrons. This component is damped relatively slowly (as x^{-2}). In view of such a complicated form of the field, the concept of the penetration depth does not have the same significance as for the normal skin effect. The complicated field profile is caused by the thermal motion of electrons. Electrons that have acquired momentum from the field in the skin layer carry this momentum into the interior of the plasma to a distance of the order of the mean free path and generate a high-frequency current on the way. Since the electrons escaping

into the plasma bulk acquire a much smaller amount of energy from the field than the 'glancing' electrons and since the current density is spread over a layer whose thickness is not δ but λ, both the current density and the field in the bulk are considerably weaker than they are in the skin layer and decay to zero at a depth of the order of the electron mean free path. Thus, even in the simplest case, the damping of the field is characterized by two quantities (δ and λ) of different orders of magnitude.

In a spatially inhomogeneous plasma, the shape of the plasma boundary is governed by the profile of the electrostatic potential $\phi(x)$ at the boundary. A theory for the anomalous skin effect in a plasma with a diffuse boundary ($\phi(x)$ is not a square well) was constructed in [21, 23].

4. The influence of a static magnetic field

The application of a static magnetic field gives rise to several new physical effects [4]. Qualitatively, the role of the magnetic field can be understood in terms of an effective conductivity σ_{eff}. It is known that an electron subjected to a static magnetic field moves along a helix of radius $r_H = mv_\perp/eB$ whose axis is parallel to the magnetic field. For a magnetic field along the z-axis, the conductivity tensor in the *bulk* plasma is [25]

$$\hat{\sigma} = \begin{pmatrix} \sigma_{xx} & \sigma_{xy} & 0 \\ -\sigma_{yx} & \sigma_{yy} & 0 \\ 0 & 0 & \sigma \end{pmatrix}. \tag{24}$$

The field does not affect the longitudinal component of the conductivity, $\sigma_{zz} = \sigma$. However, the transverse components of the conductivity $\sigma_{xx} = \sigma_{yy} = \sigma/(1+\omega_H^2/\nu^2)$ decrease with increasing B and become very small for $\omega_H \gg \nu$: $\sigma_{xx} = \sigma_{yy} \sim \sigma(r_H/\lambda)^2$.

The conductivity near the *surface* may be quite different from (24). Consider a magnetic field parallel to the boundary. If electrons are scattered diffusively by the boundary (typical for metals), momentum is lost in each collision with the boundary. Therefore, the effective collision frequency of electrons in a layer of thickness r_H is equal to the gyrofrequency $\omega_H \gg \nu$. Consequently, within the surface layer, we have for large B

$$\sigma_{xx}^s \approx \sigma \frac{r_H}{\lambda} \gg \sigma \left(\frac{r_H}{\lambda}\right)^2 = \sigma_{xx}. \tag{25}$$

Thus the *surface* conductivity is larger than the bulk conductivity. A considerable rise in the conductivity within the boundary layer compared to the bulk conductivity results in concentration of the current near the boundary, a phenomenon known as the *static skin effect* in metals [4]. In the case of specular reflection from the boundary (typical for discharge plasma), collisions with the surface do not lead to scattering. The electrons in the boundary layer follow infinite paths and the *surface* conductivity is even larger, of the order of the bulk conductivity without magnetic field. In any case, the principal contribution to the total current is made by a surface layer of thickness r_H.

The current practically vanishes at $x > r_H$ and the field and current have different depths of penetration.

Analysing the influence of a static magnetic field parallel to the boundary, we can distinguish two limiting cases with respect to the frequency of the alternating field.

(1) When the frequency of the alternating field is relatively low, $\omega \ll \nu$, the alternating field does not change significantly during the time ν^{-1}. Electrons spend different times in the skin layer, depending on the angle at which they enter the skin layer. The 'glancing' electrons, which are the only ones of importance for the anomalous skin effect, travel a path of length $\sim\sqrt{r_H\delta}$ during the field period. If

$$\sqrt{r_H\delta} \gg \lambda \qquad (26)$$

all 'glancing' electrons traverse the greatest possible distance (of the order of λ) in the skin layer without suffering collisions. Thus, the magnetic field does not affect the impedance.

When the magnetic field is increased that so that

$$\sqrt{r_H\delta} \ll \lambda \qquad (27)$$

although we still have $r_H \gg \lambda$, the glancing electrons traverse a path of the order of $\sqrt{r_H\delta} \ll \lambda$ in the skin layer and this reduces the conductivity by a factor of $\sqrt{r_H\delta}/\lambda$. The relative number of 'glancing' electrons is $\delta/\sqrt{r_H\delta}$. Thus, the effective conductivity

$$\sigma_{eff} = \sigma \frac{\sqrt{r_H\delta}}{\lambda} \frac{\delta}{\sqrt{r_H\delta}} = \sigma \frac{\delta}{\lambda} \qquad (28)$$

is of the same order as that given by (14) in the absence of the magnetic field! If the magnetic field is parallel to the surface the effective conductivity is larger than that given by (28) by a factor equal to the number of times that an electron returns to the skin layer during the time ν^{-1}, i.e. by a factor of $\lambda/2\pi r_H$:

$$\sigma_{eff} \approx \sigma \frac{\delta}{2\pi r_H}. \qquad (29)$$

Consequently, the impedance (16) has to be multiplied by $(\lambda/2\pi r_H)^{-1/3}$

$$\zeta(B) = \zeta(0) \left(\frac{\lambda}{2\pi r_H} \right)^{-1/3} \qquad (30)$$

where $\zeta(0)$ is the impedance in the absence of a magnetic field. In the low-frequency case, an electron repeatedly entering the skin layer finds that the field is practically constant.

(2) At relatively high frequencies, $\omega \gg \nu$, one has to simply replace ν by $i\omega$ in the calculations of the effective conductivity. In this case, there is no dissipation of energy in the absence of a boundary. However, if $\omega_H < \omega$, electrons can be continuously accelerated by the field and a specific cyclotron resonance may occur.

It is well known that a free electron subjected to a static magnetic field and a circularly polarized electric field experiences a resonance at $\omega = \omega_H$. Due to strong
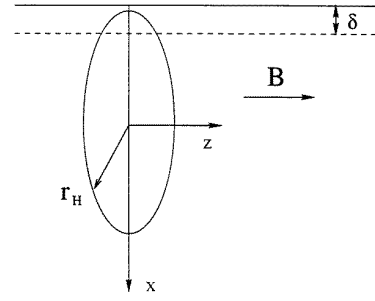
Figure 5. Electron trajectories in a magnetic field parallel to the plasma boundary for $\delta \ll r_H$. Electrons passing the skin layer congregate at a depth $\approx 2r_H$ giving rise to a local peak of current density there.

inhomogeneity of the electromagnetic field over distances of the order of an orbit radius, appreciable resonance can be observed only if an electron makes at least several revolutions between two successive collisions. This means the inequalities $\omega \gg \nu$ and $\lambda > r_H$ must be satisfied and the skin depth must be of the order of c/ω_H. If the field is inclined to the surface, practically all electrons escape from the skin layer in the first revolution. If the field is parallel to the surface, there are some electrons which do not collide with the surface and return to the skin layer after each revolution. In this case, the skin layer plays a role completely analogous to the accelerating gap in a cyclotron. If the return of electrons to the skin layer is synchronized with the external high-frequency field and the frequency ω is equal to or a multiple of the frequency ω_H, electrons are accelerated in the skin layer by a factor $\lambda/2\pi r_H$. This gives rise to a special type of cyclotron resonance known as Azbel–Kaner resonance in metals. A similar resonance has been recently discussed for a discharge plasma [28].

When a static magnetic field is parallel to the plasma boundary, the damping of a high-frequency field is of special nature. In a layer of thickness δ, electrons acquire directed velocity and give rise to a current density j. Moving down along their orbit, the electrons 'congregate' again in a layer of thickness δ at a depth $\approx 2r_H$ (see figure 5). The current density has a local maximum at that point and has opposite sign compared to that in the skin layer. Therefore, if all electrons were to move along orbits of the same radius, the 'glancing' electrons would give rise to peaks of the current and electromagnetic field at a depth $x = 2r_H$. Such peaks would accelerate new electrons which have 'glanced' in the layer at a depth $2r_H$, and this would be repeated at $4r_H$, etc. Due to the presence of orbits of different radii r_H, only a small fraction of electrons 'congregates' at any given depth and the amplitude of field spikes decreases rapidly at each 'stage'. The appearance of such field and current peaks gives rise to several macroscopic effects which have been unambiguously proven in metals [4]. The physical origin of the field (current) peaks implies that they should be observed any time when there is a mechanism selecting a small fraction of electrons whose orbit-diameter scatter is of the order of or less than the skin depth.

The theory of the anomalous skin effect in a plasma with a diffuse boundary located in a magnetic field was

developed in [22] and [23]. In [22], the static magnetic field was parallel to the boundary. Consideration was restricted to the extremely anomalous skin effect when the skin depth δ_a was small compared to the average Larmor radius of electrons and the thickness of the boundary a. An integral equation for the electric field in the plasma was obtained in the form

$$\frac{d^2 E}{dx^2} = \frac{i \coth(\pi\beta)}{\delta_a^2} \int_{-\infty}^{\infty} \exp\left\{-\frac{-e[\phi(x) + \phi(x')]}{2T_e}\right\}$$
$$\times K_0\left(\frac{e|\phi(x) - \phi(x')|}{2T_e}\right) E(x') \, dx' \qquad (31)$$

where $\beta = (i\omega + \nu)/\omega_H$ and $K_0(x)$ is a modified Bessel function. Equation (31) differs from the similar equation with no magnetic field [21] only by the factor $\coth(\pi\beta)$. This factor accounts for electron revolutions into the skin layer with frequency ω_H. Equation (31) was solved in [22] for an exponential profile of plasma density at the boundary, $n(x) \propto \exp(x/a)$, for $\ln(a/\delta) \gg 1$. In this case the wave attenuates strongly in the skin layer and does not reach the region where the plasma density begins to deviate from exponential. The real part of the surface impedance was obtained in the form

$$\zeta'(B) = \frac{2\pi^2 a\omega}{c^2}\left[1 - \frac{2}{\pi}\tan^{-1}\left(\frac{\sin(2\pi\omega/\omega_H)}{\sinh(2\pi\nu/\omega_H)}\right)\right]. \quad (32)$$

Consider the dependence of ζ' on B. In the absence of a magnetic field,

$$\zeta'(0) = 2\pi^2 a\omega/c^2. \qquad (33)$$

For a weak magnetic field, when $\omega_H \ll \nu$, the surface resistance differs from its value without the magnetic field by an exponentialy small oscillating addition

$$\zeta'(B) = \zeta'(0)\left[1 - \frac{4}{\pi} e^{-2\pi\nu/\omega_H}\sin\frac{2\pi\omega}{\omega_H}\right]. \qquad (34)$$

In the region $\omega_H \approx \omega \gg \nu$, the surface resistance is a periodic function of ω, and the ratio $\zeta'(B)/\zeta'(0)$ is closer to being rectangular in shape the better the inequality $\omega_H \gg \nu$ holds true (figure 6). The jumps of the resistance at $\omega = (m + 1)\omega_H$, where m is an integer, are connected to the Azbel–Kaner resonance, when an electron has the same phase as the field after each revolution. The jumps at $\omega = (m + 1/2)\omega_H$ occur because the phase difference between the electron and the field is exactly reversed. This is a 'cyclotron antiresonance' [22]. In the region of stronger magnetic fields, for which $v_T/a \ll \omega_H \ll \omega$, the surface resistance does not depend on the magnetic field: $\zeta' = (4\pi a\omega/c^2)\tan^{-1}(\nu/\omega)$. With further increase of B, the Larmor radius of electrons becomes smaller than δ and the conditions of the anomalous skin effect are violated.

The case of a magnetic field perpendicular to the boundary was analysed in [23]. In this case, the insident wave breaks into a sum of right and left circularly polarized components which propagate independently of one another. The interaction of the wave that rotates in the same direction as the electrons in the magnetic field has a resonant character at a field frequency close to the Doppler-shifted cyclotron frequency of the electrons [8].
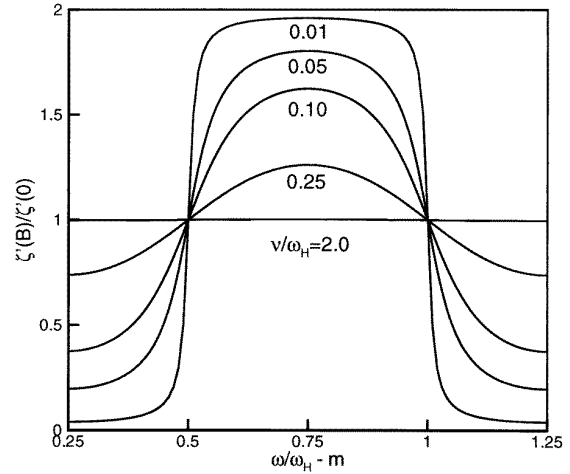
Figure 6. The ratio of surface resistance $\zeta'(B)$ in a magnetic field to its value at $B = 0$ for a semi-infinite plasma with a diffuse boundary [22]. The static magnetic field is parallel to the boundary.

5. Anomalous skin effect in bounded plasmas

The presence of a second boundary influences the skin effect if the distance between the boundaries, L, satisfies the conditions $L < \lambda$, or $L < \delta$. For metals this property is called the size effect [29]. Application of a static magnetic field B parallel to the boundary produces a very interesting effect in thin metal films. If the thickness of the film L obeys $\delta \ll L \ll \lambda$ then the application of a B field exceeding a critical value B_c confines all orbits so that electrons return repeatedly to the skin layer. Consequently, a kink in the derivative of the surface impedance with respect to the magnetic field is observed at $B = B_c$. The presence of field and current peaks discussed in section 4 results in resonant behaviour of the surface impedance in thin metal films. Discontinuities in the behaviour of the surface impedance are an unambiguous proof of the existence of these peaks [4].

In discharge plasmas, the electromagnetic fields are spatially inhomogeneous even in the absence of skin effect ($\delta > L$) due to the finite size of the coil producing the rf fields or the influence of metallic boundaries. Thus it is necessary to distinguish the field shielding by the plasma from the effects of geometry. A typical gas discharge with pronounced skin effect is an electrodeless 'ring discharge' invented more than a century ago [30] (figure 7). In this discharge, a time-varying magnetic field, B_z, produced by the rf current in the coaxial coil generates a solenoidal electric field E_θ which sustains a plasma. The E_θ field vanishes on the discharge axis due to azimuthal symmetry. The plasma is radially inhomogeneous due to the charged particle flow to the wall, and a static space charge field builds up to balance the escape rate of mobile electrons and heavy ions. This field confines the majority of electrons in the plasma. The trapped electrons are specularly reflected by the potential barriers at the plasma–sheath boundaries. The finite dimension of the plasma becomes particularly important for electron kinetics when the characteristic length (radius of the chamber) is comparable to or less than
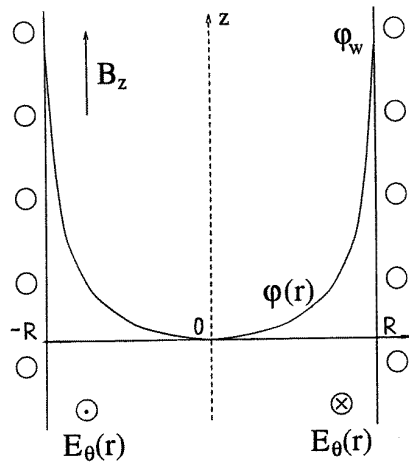
Figure 7. A sketch of an inductive discharge sustained by a coaxial coil. A time-varying magnetic field B_z induces a solenoidal electric field E_θ. The electrostatic potential $\phi(r)$ confines the majority of electrons in the plasma.

Figure 8. Axial profile of the amplitude and phase of the rf magnetic field in a planar plasma slab. Plasma parameters: $2\omega/\bar{\Omega} = 1.5$; $2\nu/\bar{\Omega} = 0.3$; (a) $L/\delta_p = 4.0$; (b) $L/\delta_p = 4.5$ [13]. Here $\bar{\Omega}$ is the mean bounce frequency, L is the half-thickness of the slab, and δ_p is the collisionless skin depth.

the electron mean free path. In this case, the momentum gained by electrons from the electromagnetic forces in the skin layer is transferred by thermal motion to the opposite layer where the momentum may lead or lag the phase of the applied field, depending on the field frequency and transit time of electrons. The finite-size effects and transit-time resonances have been studied in a number of works.

5.1. Classical works on the anomalous skin effect in discharge plasmas

Demirkhanov *et al* [9] were the first to measure a non-monotonic distribution of the rf magnetic field in a toroidal ring discharge. They explained the non-monotonic decay of the field by the thermal motion of electrons transferring rf current from the skin layer into the interior of the plasma. Also they pointed out the possible influence of the rf magnetic field and the finite dimensions of the plasma on the nature of the skin effect. Their work [9] triggered further studies of the anomalous skin effect in gas discharge plasmas.

Weibel [10] extended the Reuter–Sondheimer theory [7] for a semi-infinite uniform plasma with a Maxwellian EDF. He found a non-monotonic distribution of the rf electric field (see figure 3) and introduced the fundamental parameter Λ as a measure of non-locality of electromagnetic phenomena in plasmas. He pointed out that in the extreme anomalous case neither the skin depth δ nor the surface impedance ζ depend on the collision frequency and the dissipation of energy is present even if $\nu = 0$.

Kofoid [11] compared the result of his measurements of the anomalous rf magnetic field penetration in a cylindrical inductive discharge with Weibel's theory. He found fair agreement with theoretical predictions and attributed the major source of discrepancy to the effect of cylindrical geometry and inhomogeneity of the plasma not accounted for in the theory.

Reynolds *et al* [12] measured the penetration of electromagnetic fields into a cylindrical plasma under conditions where the electron mean free path is comparable with the plasma diameter, in the frequency range 0.1–10 MHz. In their experiments, a mercury plasma was sustained by a steady current. An rf magnetic field $\sim$0.5 G induced by a screened coaxial solenoid had negligible influence on the plasma parameters. It was found that the ratio of the amplitude of the alternating magnetic field at the plasma boundary to that at the plasma axis exhibits a maximum, particularly pronounced at a critical frequency of 4.5 MHz. This behaviour was attributed to the thermal motion of electrons, with the critical frequency being related to the transit time for electrons crossing the tube diameter.
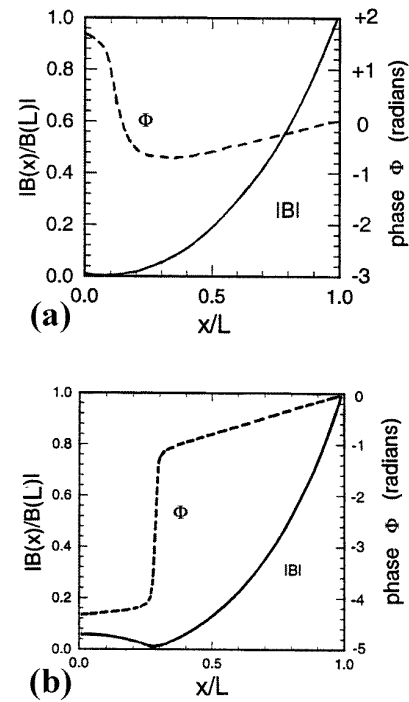
Blevin *et al* [13] developed a kinetic theory for the penetration of an electromagnetic wave into a planar plasma slab. They considered electromagnetic fields produced by two opposite current sheets placed at $x = \pm L$ (see next section where the main results of this theory are outlined). Solution of a coupled set of Boltzmann and Maxwell equations revealed pronounced resonance phenomena in the attenuation of the field at $\omega \approx \bar{\Omega}$, where $\bar{\Omega}$ is the bounce frequency of electrons with a mean velocity v_T. Non-monotonic distribution of the amplitude of the rf magnetic field and significant variations of the field phase with position were found. When a minimum of $|B(x)|$ is particularly pronounced, there is an abrupt phase change of $\approx\pi$ corresponding to the magnetic field reversal at the position of the minimum (see figure 8).

In [14] the theory was extended to a cylindrical plasma with an electrostatic potential of the form $\phi(r) =$
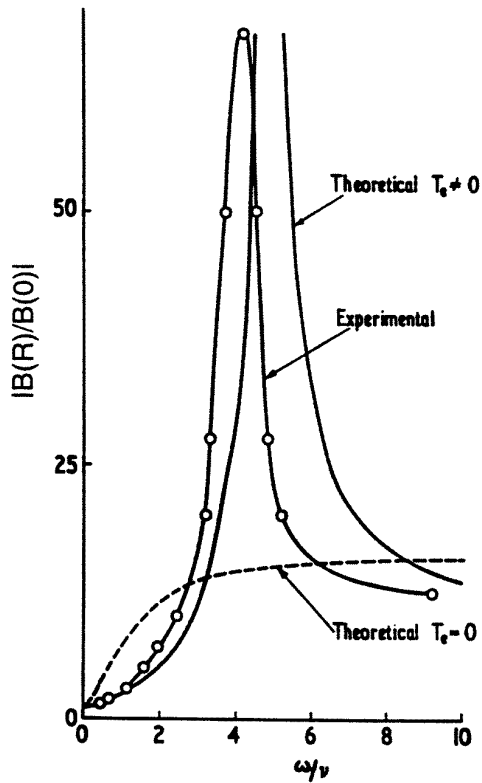
Figure 9. The ratio $|B(R)/B(0)|$ of the amplitude of the rf magnetic field at the plasma boundary to that on the axis for the first resonance [17]. Points—experiment in a cylindrical plasma, solid line—results of the kinetic theory for a planar plasma slab at $v/\bar{\Omega} = 0.3$; dashed line—'cold plasma' approximation.

Figure 10. Radial distributions of the amplitude of the rf magnetic field, $B_z(r)$ (arbitrary units) in a cylindrical plasma with a Gaussian profile of the plasma density, $n(r) \propto \exp(-r^2/a^2)$ with $a = v_T/\Omega_0$ for different values of a/δ_p (numbers near the curves). The plasma parameters correspond to $\omega_H = \Omega_0 = 2v$ and $\omega/v = 4$ [15].

$-(m/2e)\Omega_0^2 r^2$ which corresponds to a Gaussian shape of electron density, $n(r) \propto \exp(-r^2/a^2)$ with a width $a = v_T/\Omega_0$. The electron bounce frequency in such a parabolic potential well, Ω_0, is independent of electron energy. Resonant phenomena similar to those in [13] were found at ω equal to even multiples of Ω_0, in contrast to the planar geometry where resonances occur at odd multiples of $\bar{\Omega}$. Experimental measurements of the radial profile of the magnetic field were also performed. The comparison of experimental measurements of the magnetic field with calculation results revealed qualitative agreement. The quantitative discrepancies were attributed to the differences of the potential profiles in the theory and the experiments.

A comparison of theory with experiments was also given in [17]. Experiments were performed in a cylindrical tube 150 cm long with radius $R = 4$ cm containing mercury vapour at pressures 0.1–1 mTorr. The alternating fields were produced by rf current in a coaxial screened solenoid. The azimuthal electric field induced by the time-varying magnetic field was small compared to the axial dc electric field maintaining the plasma. The amplitude and phase of the magnetic field were measured by magnetic probes. Figure 9 shows the main results. The penetration of electromagnetic fields exhibits sharp resonances at particular values of electron density, excitation frequency, and plasma radius. The first resonance (shown in figure 9) agreed well with the plasma
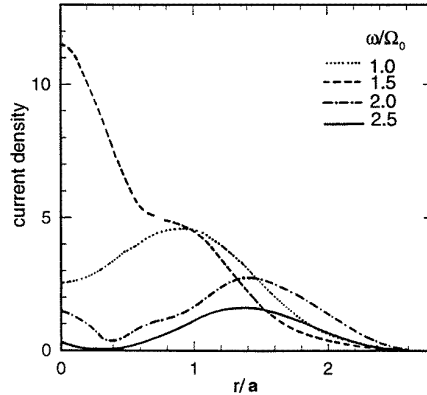
Figure 11. The radial distribution of the rf current density (arbitrary units) in a cylindrical plasma with a Gaussian profile of the plasma density, $n(r) \propto \exp(-r^2/a^2)$, where $a = v_T/\Omega_0$, for different values of ω/Ω_0. The rf electric field is directed along the axis of the cylinder [16].

slab theory. The experimentally found parameters of the second resonance (not shown in figure 9) did not agree with the predictions of the theory, for reasons that were unclear. Additional experimental measurements and attempts to fit the experimental data to the theory [14] were reported in [18].

Storer and Meaney [15] included an axial static magnetic field in the theory of the anomalous skin effect in a cylindrical plasma. They pointed out that in the presence of a static magnetic field, it is necessary to consider the radial
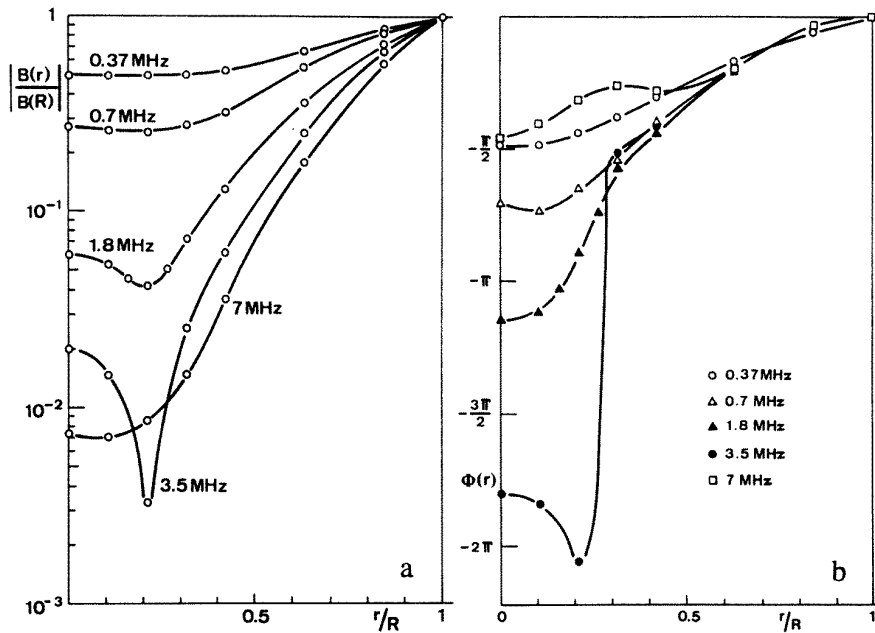
Figure 12. The radial distributions of the amplitude (a) and phase (b) of the rf magnetic field for different driving frequencies in a cylindrical argon plasma. Plasma parameters: 10 mTorr, $n_e = 3.6 \times 10^{12}$ cm^{-3}, $T_e = 2.1$ eV [19].

electric field in addition to currents and electric field in the azimuthal direction. In the cold-plasma approximation, the fields adjust themselves so that the static magnetic field does not affect E_θ. However, even for the cold plasma, the static magnetic field results in a non-zero component of the electric field in the radial direction. Recently, this point was raised in [31]. Storer has found that even a small change in the static magnetic field may lead to complex redistributions of the alternating fields when the Larmor radius of the electrons is comparable to the size of the plasma (figure 10). The anomalies in the radial distribution of the rf magnetic field are even more pronounced than without a static field. There can be considerable enhancement in the field on the axis (see figure 10). No experimental data were available to compare with the theory.

In [16] the theory of the anomalous skin effect in a bounded cylindrical plasma was extended to the case of an rf electric field parallel to the axis of the column. This situation is complimentary to the aforementioned case of the azimuthal electric field. Similar resonance phenomena were found in this case as well. Figure 11 shows the relative magnitude of the current density profiles for various values of ω/Ω_0. The anomalous current in the centre appears at $\omega/\Omega_0 = 1.5$. Two current layers are seen at $\omega/\Omega_0 = 2.0$ and $\omega/\Omega_0 = 2.5$. The phase of the current density at the centre differs from that at the edge by about π, i.e. the current at the centre is in the opposite direction to the local rf field. No experimental data were presented in [16].

Systematic experimental measurements and comparison with available theories were performed by Joye and Schneider [19] in a cylindrical argon plasma with and without static axial magnetic field. The driving frequency varied in the interval 0.32–14 MHz, and the plasma density was between 10^{12} and 10^{13} cm^{-3} in a tube of radius $R = 4.7$ cm at a pressure of 10 mTorr. Typical experimental
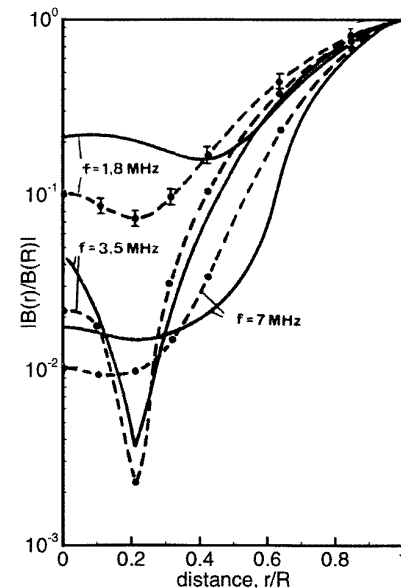
Figure 13. The radial distributions of the amplitude of the rf magnetic field in a cylindrical argon plasma. Dotted lines show experimental data for $p = 10$ mTorr, average plasma density $n = 4.2 \times 10^{12}$ cm^{-3}, and $T_e = 2.1$ eV. Solid lines are calculations according to the Sayasov theory for $n_e = 3 \times 10^{12}$ cm^{-3}, $\nu = 4 \times 10^7$ s^{-1} [19].

results are shown in figure 12. It is seen that an off-axis minimum of the magnetic field is observed at a particular driving frequency. This local minimum vanishes both at low and high frequencies. Also, an abrupt change of the field phase takes place in the position of the minimum (figure 12(b)). The Sayasov theory described below fits the data best (see figure 13). The influence of a static magnetic field, B_0, is illustrated in figure 14 for a frequency 3.5 MHz.
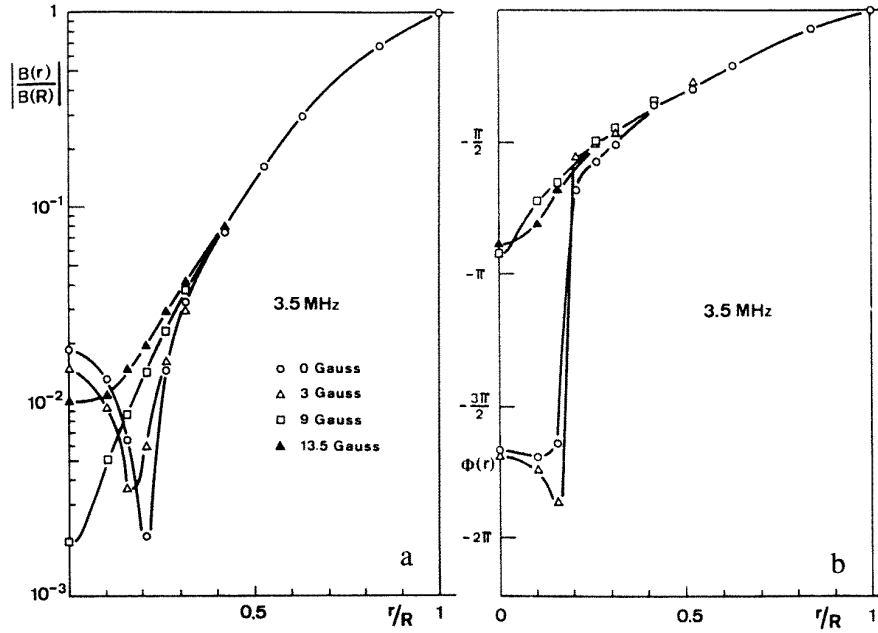
Figure 14. Radial distributions of the amplitude and phase of the rf magnetic field in a cylindrical argon plasma for different values of an axial static magnetic field. Plasma parameters: 10 mTorr, $n_e = 3.4 \times 10^{12}$ cm^{-3}, $T_e = 2.1$ eV, $\omega/2\pi = 3.5$ MHz [19].

The off-axis minimum of $|B(r)|$, observed without static magnetic field, gradually disappears with an increase of B_0. A field as weak as $B_0 = 3$ G already modifies the position of the local minimum (this field corresponds to $\omega_H/2\pi = 8.4$ MHz, $r_H = 1.6$ cm). The off-axis minimum disappears at $B_0 = 9$ G when $r_H = 0.53$ cm. The effect of the static magnetic field is more pronounced when the fundamental parameter Λ reaches a maximum (figure 2).

Sayasov [20] developed an analytic theory for the skin effect in a cylindrical plasma under conditions $\delta \ll R$, $\lambda \ll R$ which are frequently satisfied in experiments. This theory will be briefly described in the following section. A comparison of the theory with the experiments given in figure 13 demonstrates a fairly good agreement. The remaining discrepancies can be attributed to the approximation of a rectangular potential profile $\phi(r)$ employed in the theory.

The theory of the anomalous skin for an arbitrary profile of $\phi(x)$ was developed in [21–23]. To our knowledge, this theory has not been compared to experiments yet.

The classical works on the anomalous skin effect described above pay little attention to the analysis of electron heating. The influence of the rf magnetic field on electron dynamics is ignored. Theory is restricted to the linear case and to conditions when electron collisions with neutral gas species are responsible for randomizing the electron motion. Under these circumstances the effect of the rf magnetic field can be neglected. The self-consistent nature of a discharge is frequently ignored; the electron distribution function is assumed to be Maxwellian with electron temperature being an input parameter. In the next section we shall describe in more detail the available theories of the anomalous skin effect in bounded discharge plasmas.

5.2. Basic theories

Following [13], consider the electromagnetic fields produced by two symmetric current sheets placed at $x = \pm L$. Assume that all quantities vary with angular frequency ω, the magnetic field, $B_z(x) = (c/i\omega)\,dE_y/dx$ is symmetric and the electric field $E_y(x)$ is antisymmetric about $x = 0$:

$$E_y(x) = \sum_n \alpha_n \sin\left[\frac{\pi n x}{2L}\right]. \qquad (35)$$

Here the summation extends over odd values of n. An electrostatic potential forms a rectangular potential well with sharp boundaries (thin sheaths) at $x = \pm L$ specularly reflecting electrons. The electrons reflected from the boundaries can be regarded as entering the plasma from $|x| > L$. In such a way the problem is reduced to that for an infinite plasma with spatially periodic fields (see figure 15).

The EDF is approximated as the sum of a time-independent isotropic part $f_0(\varepsilon)$ and an oscillating part, f_1. If the amplitude of the applied field is small, the linearized Boltzmann equation can be used to calculate f_1. Neglecting the effect of the rf magnetic field on electron motion, one obtains

$$
f_1 = -ev_y \frac{\partial f_0}{\partial \varepsilon}
$$
$$
\times \sum_n \alpha_n \frac{(i\omega + \nu)\sin(\pi n x/2L) - n\Omega\cos(\pi n x/2L)}{(i\omega + \nu)^2 + (n\Omega)^2}
$$
$$(36)$$

where $\Omega = \pi v_x/2L$ is the bounce frequency of an electron with velocity v_x. Equation (36) indicates that at $\nu \ll \omega$, f_1 becomes anomalously large for resonance electrons for which the bounce frequencies satisfy $\omega = n\Omega$. Assuming a
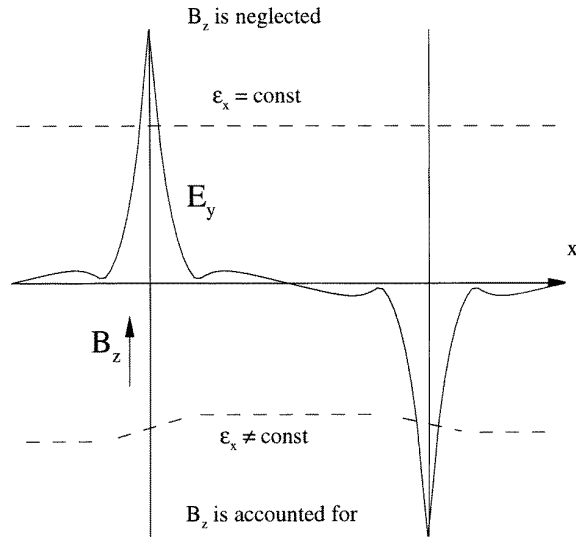
Figure 15. Collisionless electron motion in a plasma slab is identical to the motion in an infinite plasma with spatially periodic fields. With neglect of the rf magnetic field, velocity kicks are in the direction of the electric field (y-direction) and the energy along the x-axis, ε_x, remains constant (top). Accounting for the rf magnetic field results in velocity kicks in the x-direction and in a change of ε_x (bottom).

Figure 16. Spatial distributions of the amplitude and phase of the rf magnetic field in a planar slab for $\Lambda = 3.7$, $\omega/\nu = 5$, $\epsilon = 15°$. Solid lines are calculated according to equation (35), dotted lines are calculated using the formula (43) [20].
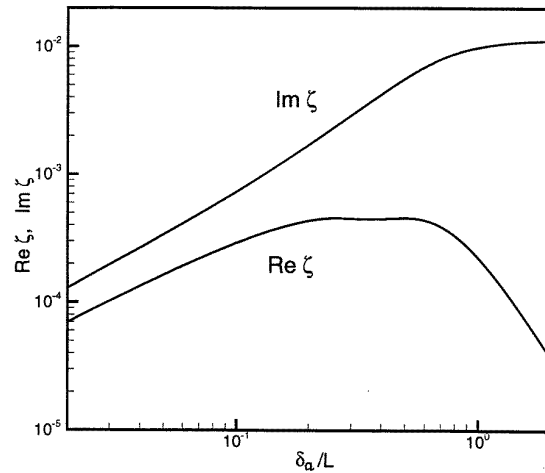
Figure 17. The real and imaginary parts of the surface impedance of a plasma slab as functions of δ_a/L calculated according to equation (39). The plasma parameters are: $\nu/\omega = 0.01$, $R = 4$ cm, $\omega = 8.5 \times 10^7$ s^{-1}, $T_e = 5$ eV.

Maxwellian distribution for $f_0(\varepsilon)$, the current density can be expressed in the form [13]

$$j_y(x) = -\frac{in_e e^2}{m v_T} \sum_n \frac{\alpha_n}{(\pi n/2L)} \sin(\pi n x/2L) Z(\xi/n). \quad (37)$$

Here $Z(\xi)$ is the plasma dispersion function, $\xi = (i\nu - \omega)/\bar{\Omega}$, and $\bar{\Omega} = \pi v_T/2L$ is the mean bounce frequency for electrons with the most probable speed $v_T = (2T_e/m)^{1/2}$. The solution of Maxwell's equations with the current density (37) gives for $\omega \ll \omega_p$ the Fourier coefficients

$$\alpha_n = -\frac{2Li\omega B_0 \sin(n\pi/2)(\pi/2)^{-2}}{n^2 + (2L\omega_p/\pi c)^2[\omega Z(\xi/n)/n\bar{\Omega} + (L/R_{eff})^2]} \quad (38)$$

where B_0 is the amplitude of the magnetic field at $x = \pm L$. Bearing in mind a later comparison with experiments for radially inhomogeneous plasma, we have added a term, $(L/R_{eff})^2$, which would appear in the denominator of the solution to a two-dimensional cylindrical problem, R_{eff} being an effective radial scale. The non-symmetric case is treated in [8] and [46].

Using these results, the surface impedance of the plasma slab ($R_{eff} \to \infty$) can be found in the form

$$\zeta = \frac{i\omega}{c} \frac{E(L)}{E'(L)} = \frac{8i\omega L}{\pi^2 c}$$
$$\times \sum_n \frac{1}{n^2 + (2L\omega_p/\pi c)^2(\omega Z(\xi/n)/n\bar{\Omega})}. \quad (39)$$

In limiting cases, this expression can be simplified. At $L \gg c/\omega_p$, one obtains the surface impedance of a slab without plasma

$$\zeta = \frac{i\omega L}{c}. \quad (40)$$

In the 'cold-plasma' approximation ($v_T = 0$) using the asymptotic expansion $Z(\xi) \approx -1/\xi$ for $|\xi| \gg 1$, one obtains (see, for example, p 44 of [32])

$$\zeta = \frac{i\omega}{\omega_p} \sqrt{\frac{\nu + i\omega}{i\omega}} \tanh\left[\frac{\omega_p L}{c} \sqrt{\frac{i\omega}{i\omega + \nu}}\right]. \quad (41)$$

This result can be obtained alternatively [33] by solving equation (6) with σ given by (10). For a thick plasma slab, when $\lambda_{eff} \ll L$ and $\delta \ll L$, the theory should give the results of section 3.2 for a semi-infinite plasma.

Sayasov has shown that the series in (35) allows summation by the method of complex integration. At $\Lambda > 1$, the distribution of electromagnetic fields in the plasma slab can be represented as a superposition of three fundamental modes

$$B(x) \approx B_0 \sum_1^3 A_n \frac{\cos(k_n \tilde{x})}{\cos(k_n L)} \quad (42)$$

where $\tilde{x} = x/L$, k_1, k_2, and k_3 are the three complex roots of the equation $D(k) = k^2 + \Lambda Z(\mathrm{i}s/k)/k = 0$, and $A_n = k_n/D'(k_n)$ where the prime refers to the first derivative. For $\Lambda \gg 1$, the two roots k_2 and k_3 are located symmetrically relative to the imaginary axis, and the field profile becomes particularly simple

$$B(x) \approx \frac{B_0}{3}\left[\frac{\cosh k\tilde{x}}{\cosh k} + 2\,\mathrm{Re}\,\frac{\cos(k\,\mathrm{e}^{\mathrm{i}\pi/6}\tilde{x})}{\cos(k\,\mathrm{e}^{\mathrm{i}\pi/6})}\right]. \qquad (43)$$

Here $k = \pi^{1/6}\Lambda L/\lambda_{eff}$. Equation (43) reproduces the essential features of the complete solution (35) (see figure 16).

In the limit $L \gg \lambda_{eff}$, Sayasov obtained a simple expression for the surface impedance†

$$\zeta = \frac{4}{3^{3/2}}\frac{\omega\lambda_{eff}}{c\Theta}\left[\mathrm{e}^{\mathrm{i}\pi/3} + \frac{4\mathrm{i}}{3\pi^{1/2}\Theta}\,\mathrm{e}^{\mathrm{i}(\pi/6-\epsilon)} + \frac{3^{3/2}}{4\pi}\left(\frac{\mathrm{e}^{-\mathrm{i}\epsilon}}{\Theta}\right)^2\right.$$
$$\left. \times \ln\left[\gamma\left(\frac{\mathrm{e}^{-\mathrm{i}\epsilon}}{\Theta}\right)^2\right]\right] \qquad (44)$$

where $\gamma = 0.577$ is Euler's constant and $\Theta = \pi^{1/6}\Lambda^{1/3}$. For $\lambda/\delta_p \ll 1$, this expression reproduces fairly well Weibel's results shown in figure 4. According to (44), the maximum value of $\mathrm{Re}\,\zeta$ for $\lambda/\delta_p \to \infty$ is $0.123 v_T/c$ at $\omega = \omega_{max} = 0.721\nu$. Thus, for the anomalous skin effect, the energy absorbed by the plasma, is larger as compared with the normal case by the factor $(v_T/c)/(\nu/\omega_p) = \lambda/\delta_p$ [20].

In figure 17, the real and imaginary parts of the surface impedance (39) are plotted versus δ_a/L in the collisionless case, $\nu = 0$, for $\omega = 8.5 \times 10^7\,\mathrm{s}^{-1}$ (13.56 MHz). It is seen that the real part of the impedance is much smaller than the imaginary part, i.e. the effective resistivity of the plasma slab is small compared to its inductance. The electrons simply oscillate in the rf electric field without gaining much net energy. At $\delta_a/L \ll 1$ (the high-density limit) the ratio of the real and imaginary parts approaches a constant value. At $\delta_a/L > 1$ the impedance corresponds to that of a slab with no plasma (40). The maximum of the real part, $\mathrm{Re}\,\zeta$ as a function of δ_a/L, defines the optimum conditions for power transfer to the plasma. The maximum energy which can be absorbed by the plasma always remains small, since $v_T \ll c$.

The theory of the anomalous skin effect in a plasma slab with diffuse boundaries was developed in [22]. It was assumed that the alternating field does not penetrate deeply into the interior of the plasma and is essentially attenuated at a distance $a \ll L$ from the boundary. Under these conditions, it is sufficient to know the potential $\phi(x)$ only at the tail of $n_e(x)$ since low-energy electrons, moving with conservation of total energy, do not penetrate into the skin layer. The authors assumed that the electron density decays exponentially at the boundary of the plasma. For this case, the equation for the electric field is cast in the form (31) with the only substitution $\beta = (\mathrm{i}\omega + \nu)/\bar{\Omega}$. This expression for β differs from the one used in equation (31) in that the Larmor frequency ω_H is replaced by the bounce

† Up to terms of the order of Θ^{-2} this expression coincides with equation (22) in [10].

frequency $\bar{\Omega}$. Thus, equation (32) can be used to describe the surface impedance of the slab. In particular, it follows from equation (32) that the surface resistance is a periodic function of ω in the region $\omega \approx \bar{\Omega} \gg \nu$. This is a size effect. Indeed, in a plasma bounded on one side, an electron reflected from the boundary moves into the interior of the plasma until it collides with another particle. In the presence of a second boundary, an electron bounces between the two boundaries and visits the skin layer with a frequency $\bar{\Omega}$. The surface resistance depends on phase correlations between succesive electron interactions with the field.

For a thin plasma slab, for which $\delta_a \approx L$, it is necessary to know the potential $\phi(x)$ in the entire region of electron motion. The case $\phi(x) \propto |x|$ was considered in [22].

5.3. Cylindrical case

The influence of boundary curvature on the skin effect is conveniently investigated with cylindrical samples. Evidently, the result depends on the relation between the cylinder radius R, the electron mean free path λ and the thickness of the skin layer δ. Meierovich [34] considered the case $\lambda \gg R$. The electric field vector was parallel to the axis of a cylindrical conductor with a sharp boundary at $r = R$. For specular reflection of electrons at the boundary, the Maxwell equation for E_z was obtained in the form

$$\frac{\mathrm{d}}{\mathrm{d}\rho}\rho\frac{\mathrm{d}E_z}{\mathrm{d}\rho} = \alpha\int_0^1 K(x, x')E_z(x')\,\mathrm{d}x' \qquad (45)$$

where $\rho = r/R$, the kernel $K(x, x')$ is given by

$$K(x, y) = \int_0^\infty J_0\left(\frac{k\sqrt{1-x^2}}{x}\right)J_0\left(\frac{k\sqrt{1-y^2}}{y}\right)\mathrm{d}k \qquad (46)$$

and the only parameter, $\alpha = (R\omega_p/c)\mathrm{i}\omega/(\mathrm{i}\omega + \nu)$ is determined by the ratio of the field penetration depth to the radius of the cylinder. In the case of a strong skin effect, $\alpha \gg 1$, equation (45) can be simplified and the surface impedance obtained in the form

$$\zeta \approx \frac{4\pi}{c}\left[\left(\frac{\omega}{\omega_p}\right)^4\frac{\omega R}{c}\left(1 + \frac{\nu^2}{\omega^2}\right)\right]^{1/5}$$
$$\times \exp\left[\mathrm{i}\left(\frac{\pi}{2} - \tan^{-1}\frac{\nu}{\omega}\right)\right]. \qquad (47)$$

This dependence is essentially different from the case of a planar plasma slab. In particular, the dependence on the cylinder radius is relatively weak. In [35] the theory was further developed to include a static magnetic field directed along the axis of the cylinder.

Sayasov [20] considered another limit $\lambda \ll R$, $\delta \ll R$, with a rectangular potential well $\phi(r)$. The axial rf magnetic field B_z and azimuthal electric field E_θ were assumed to be generated by a cylindrical coil wrapped around the cylinder. It was shown that, similar to the planar plasma slab, the distribution of electromagnetic fields in a cylindrical plasma can be represented as a superposition of three fundamental modes

$$B(r) \approx B_0\sum_1^3 A_n\frac{J_0(k_n\rho)}{J_0(k_n)}. \qquad (48)$$

It is just the interference of these modes that leads to non-monotonic spatial distributions of the fields observed in the experiments (see figure 13). The analytical solutions enable one to explain peculiar features in the spatial distributions of the fields. For instance, the off-axis minimum of $|B(r)|$ appears only at particular values of $\omega \approx \omega_{max}$ and vanishes for low and high frequencies. At this frequency $\omega_{max} = \nu/\sqrt{2}$ the fundamental parameter, Λ, reaches a maximum as a function of ω (see figure 2).

6. Recent results

Recent interest in the anomalous skin effect has been generated by rediscovery of inductive discharges for semiconductor manufacturing [36]. Due to their relatively simpler design, low-pressure inductively coupled plasma (ICP) sources are considered as prime candidates for manufacturing ultra-large-scale integrated circuits. The ICP tools are capable of producing high-density plasmas at pressures as low as 0.5 mTorr. In a typical case the plasma is sustained by the rf fields generated by alternating current in a planar coil placed on top of a cylindrical chamber. These fields are spatially inhomogeneous even in the absence of a skin effect, due to the finite sizes of the coil and the chamber. For typical plasma densities the field shielding by the plasma is noticeable as well. The self-consistent nature of the discharge makes its modelling a formidable task. Some basic questions remain poorly understood, and in many cases empirical approaches to ICP source design predominate. There is a need for better understanding of the discharge physics to facilitate computer-aided design of plasma sources.

Turner [33] solved numerically Maxwell's equations for a plasma slab using particle-in-cell/Monte Carlo (PIC-MC) simulation of electrons to calculate the rf current density. Our calculations of the surface impedance under identical conditions using equation (39) reproduce Turner's results for $\mathrm{Re}\,\mathcal{Z}$. It is seen in figure 18 that for the considered discharge conditions, the plasma resistivity is small compared to the inductance, i.e. electrons simply oscillate in the field without gaining much net energy. Turner also found by PIC simulations that the electron current is not confined to the skin layer but spreads throughout the entire gap [37]. He suggested a modification of the fluid description of electrons that allows for such a diffusive spreading of the current and reproduces the PIC simulation results. Figure 19 shows our calculations of the electric field and current density for identical conditions using the formulae of [8] and [46]. Although a noticeable 'current diffusion' does take place, it is not so extensive as reported in [37]. Also, it is worth noting that the influence of the rf magnetic field on electron motion was neglected in Turner's simulations that can modify the heating rate in near-collisionless regimes.

Vahedi et al [38] developed an analytic model of power deposition in ICP sources. The power deposition was calculated using an expression [39] for the surface impedance that corresponds to the classical expression for ζ obtained in [10] for a semi-infinite spatially uniform Maxwellian plasma. It was implicitly assumed that
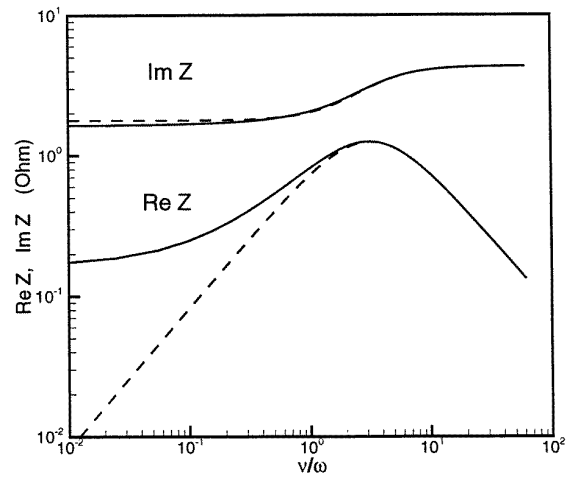
Figure 18. The real and imaginary parts of the surface impedance $\mathcal{Z} = (4\pi/c)\zeta$ for a plasma slab, shown as functions of ν/ω. The plasma parameters are: $n_e = 10^{11}$ cm^{-3}, $T_e = 5$ eV, $L = 4$ cm. The dashed lines are the cold-plasma result.
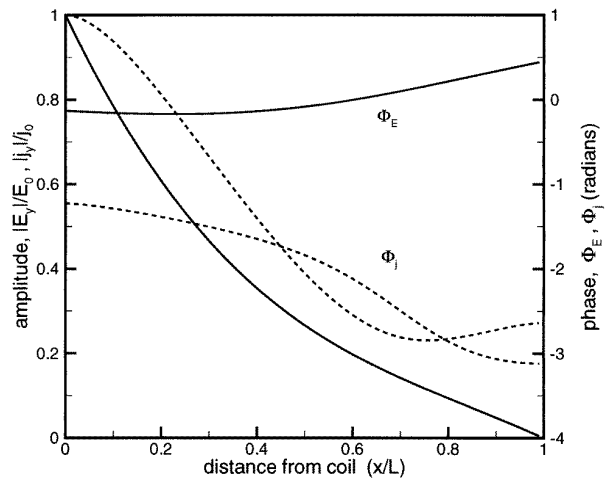
Figure 19. Axial distributions of amplitudes and phases of the rf electric field (solid lines) and current density (dashed lines). The discharge conditions are the same as in figure 18, $\omega/2\pi = 13.56$ MHz, $\nu = 0$.

electrons 'forget' the field phase due to collisions with neutrals, so that any effects of finite size of the plasma could not be predicted.

Godyak and Piejak [40] have performed precise measurements of the rf magnetic fields in a weakly collisional cylindrical ICP driven by a planar coil. The spatial distributions of the rf electric field (figure 20(a)) and electron current density (figure 20(b)) found from these measurements are nonmonotonic. The phases of the field and current change substantially with position so that the power absorption, $j \cdot E$, may be negative in the plasma bulk where the current phase differs from the phase of the local electric field by more than $\pi/2$. For comparison, figure 21 shows the results of our calculation using the formulae of [8] and [46] for the same conditions. Due to the finite size of the coil in [40] the rf field decays exponentially with a characteristic length $R_{eff} = 2.4$ cm even in the absence of

the plasma. In our calculations, this effect was taken into account by introducing the term L/R_{eff} in the formulae of [8] and [46], similar to equation (38). We did not expect a quantitative agreement with the experiment since the radial electron motion is not accounted for in equation (36) for the EDF. However, qualitatively, some experimentally observed phenomena can be described by the simple plasma slab theory. In particular, the spatial profiles of the field amplitude and phase demonstrate similar behaviour to that observed experimentally. A sudden jump of the field phase found in [40] does occur in our calculations at plasma densities $n_e \approx 2 \times 10^{11}$ cm^{-3}, twice that reported in [40]. However, the theory does not reproduce the distribution of the current density observed in [40] as accurate as the fields. Better agreement for current is obtained using higher ω in calculations. Detailed comparisons require accurate solution of the two-dimensional problem.

Some basic questions on ICP operation in the near-collisionless regime require better understanding. The first question concerns the mechanism of electron heating. Kaganovich *et al* [41] have pointed out that the finite dimension of the plasma becomes very important for electron heating in the near-collisionless regime. In a plasma slab geometry, collisionless heating (at $\nu = 0$) must be absent if the influence of the rf magnetic field on electron motion is neglected. This happens because the E_y field changes only the v_y component of the electron velocity while the v_x component remains unaffected (see figure 15, top). As a result, the bounce frequency Ω is constant and subsequent electron interactions with the E_y field are strongly correlated. Thus, v_y simply oscillates in time and electrons gain no net energy from the field. On the other hand, resonance electrons (with $\omega = k\Omega$) can make considerable contribution to the collisional heating ($\nu \neq 0$) since their v_y excursions are quite large and even rare collisions can produce considerable heating.

The second question concerns the influence of the rf magnetic field on electron kinetics and skin effect. Although the possible influence of the rf magnetic field on the anomalous skin effect in inductive discharges was pointed out more than 30 years ago [9], most of the currently used ICP models have ignored this effect. Cohen and Rognlien have recently shown [42] that the Lorentz force can greatly affect the electron motion in the collisionless skin layer. Since the canonical momentum $p_y = mv_y - eA_y(x,t)$ is a strict invariant of the collisionless electron motion (A_y is the vector potential of the magnetic field), the Lorentz force transforms a v_y kick into a v_x kick (see figure 15, bottom). Consequently, the electron bounce frequency in a plasma slab changes after each kick and collisionless electron heating becomes possible under certain conditions [41]. Gibbons and Hewett [43] performed PIC simulations of a collisionless ICP accounting for the rf magnetic field. The EDF was assumed to be Maxwellian. They found that for a planar case both components of electron velocity (v_x and v_y) were affected by collisionless heating (only v_y would have been affected if the magnetic field were not included). Collisionless heating appeared directly in these simulations. The calculated surface impedance from the PIC simulations
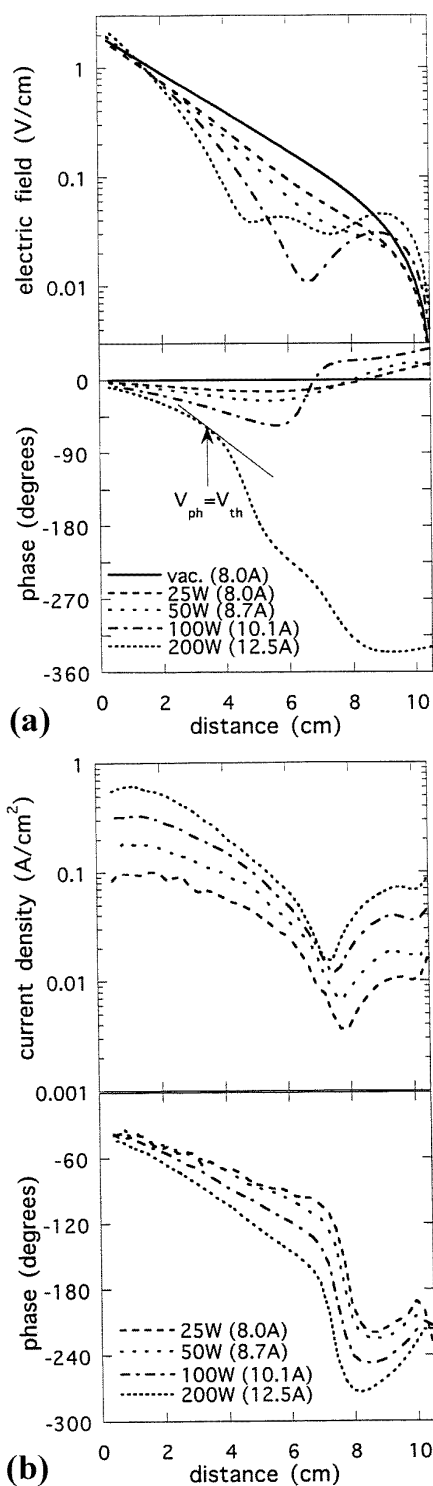
Figure 20. Experimental distributions of the rf electric field (a) and current density (b) in an ICP driven by a planar coil for different powers absorbed in the plasma [40]. Peak plasma densities were $n_0 = 2, 3.8, 6.5, 11 \times 10^{10}$ cm^{-3} as power was increased, respectively. Discharge conditions: argon, $p = 1$ mTorr, $\omega = 4.26 \times 10^7$ s^{-1}, $T_e = 5.6$ eV, $L = 10.5$ cm. The phases refer to the phase of the rf electric field in the absence of plasma.

was found in good agreement with the results of a linear kinetic theory for a semi-infinite plasma. No spatial
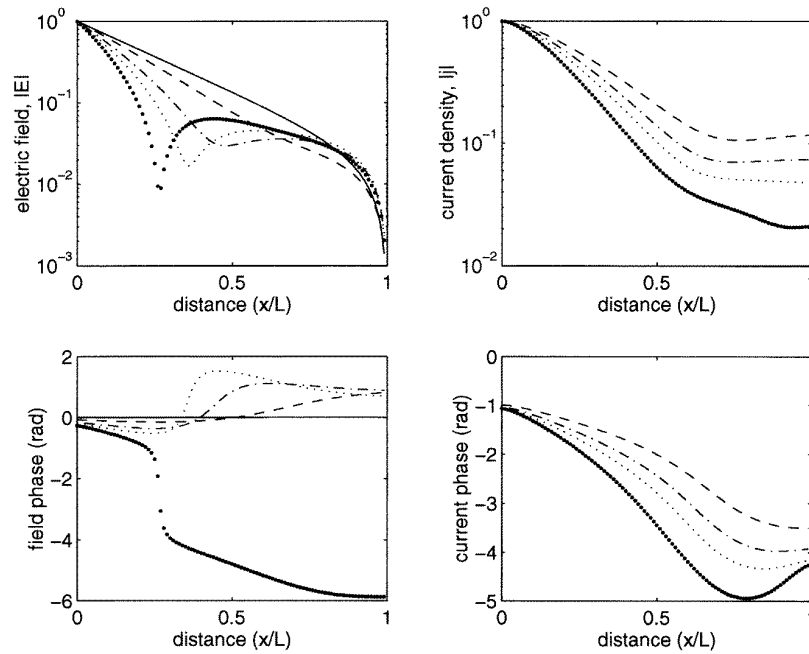
Figure 21. Amplitudes and phases of the rf electric field and current density in a plasma slab using [8] and [46] for discharge conditions similar to figure 20. Plasma densities n_e = 2, 6.5, 11, 20 × 10^{10} cm^{-3} for dashed, dash-dotted, dotted and bold dotted lines, respectively. Solid line shows the electric field distribution in the absence of plasma. Other parameters: ν = 8 × 10^6 s^{-1}, R_{eff} = 2.4 cm, ω = 4.26 × 10^7 s^{-1}, T_e = 5.6 eV, L = 10.5 cm.

distributions of the rf fields or currents were reported in [43].

Kolobov *et al* [44] have modelled the electron kinetics in a weakly collisional cylindrical ICP for a given distribution of the fields. Heating was described in terms of the energy diffusion coefficient, $D_\varepsilon = \Delta\varepsilon\,\Omega\Psi$, the product of a single energy kick in the skin layer, $\Delta\varepsilon$, bounce frequency Ω, and a function Ψ which describes the phase correlations between successive kicks. Figure 22 shows function Ψ for the 'hybrid' heating regime. In this regime, the place where electrons interact with electromagnetic fields and the place where randomizing collisions occur are spatially separated. Sharp peaks of Ψ at certain values of ω/Ω in the weakly collisional regime correspond to the bounce resonances discussed above. It was shown in [44] that averaging of D_ε over angles in velocity space diminishes the resonance effects in a cylindrical plasma. The EDF was found from a linearized Boltzmann equation and from a dynamic Monte Carlo simulation taking into account the influence of the rf magnetic field and finite dimensions of the plasma on electron kinetics. The depth of the potential well that traps the majority of electrons in the plasma was calculated self-consistently with the EDF for a wide range of pressures and driving frequencies. The role of the rf magnetic field and finite-size effects on heating and power deposition was the main focus of that work.

The role of the rf magnetic field on the skin effect becomes more important with a decrease of the field frequency ω. If we assume that a similar electric field is necessary to sustain a discharge at different frequencies, then a larger magnetic field must be created at lower frequencies. At $\omega_H \gg \omega$ the rf field can be treated as quasi-static. According to section 4, a static magnetic field
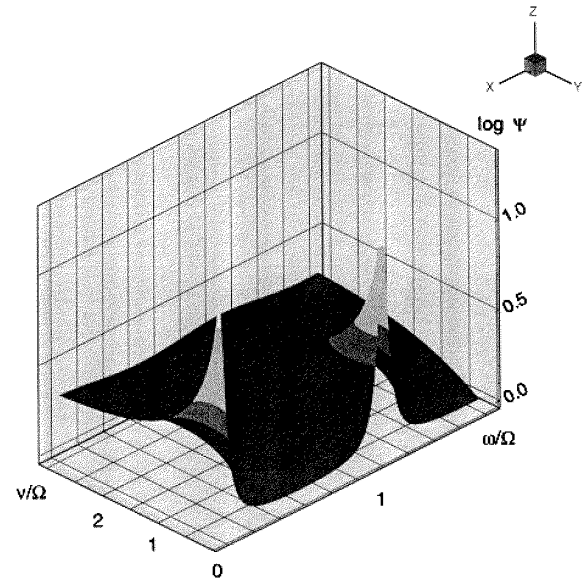
Figure 22. The function Ψ which describes phase correlations between successive electron interaction with the rf fields in a thin skin layer. Transit-time resonances are observed in the near-collisionless regime ($\nu \ll \Omega$) at $\omega = k\Omega$, where k is an integer and Ω is the electron bounce frequency.

reduces the transverse component of the conductivity tensor in the plasma bulk by a factor $(r_H/\lambda)^2$ compared to its value at $B = 0$. Qualitatively, a decrease of σ_{eff} can result in anomalously large penetration of the field when the magnetic field is accounted for in the analysis. However, as we saw in section 4, the conductivity in the skin layer

is of the order of the bulk conductivity with no magnetic field. In any case, one should expect that accounting for the rf magnetic field in the theory can substantially modify the profiles of the fields.

Tuszewski [45] has measured the penetration of the rf magnetic field in a low-pressure (5–50 mTorr) cylindrical ICP ($R = 16.5$ cm) driven by a coaxial coil at the relatively low frequency of $\omega/2\pi = 0.46$ MHz. He found enhanced penetration of the field compared to predictions of the classical models and attributed this effect to a reduction of the plasma conductivity due to the influence of the rf magnetic field on electron motion. Qualitatively, this reduction takes place when the average gyrofrequency ω_H exceeds the angular frequency ω and collision frequency ν. However, no quantitative kinetic calculations have yet been reported. The work in [46] is a good step in this direction.

In conclusion, we believe that many interesting phenomena inherent to the anomalous skin effect in metals are yet to be found in gas discharges. On the other hand, new effects associated with the nonlinear self-consistent nature of gas discharges may be discovered. Among the most important unresolved problems is the influence of the rf magnetic field and of externally applied magnetic fields on the skin effect and collisionless electron heating in bounded plasmas.

Acknowledgments

References

[1] Lifshitz E M and Pitaevskii L P 1981 *Physical Kinetics* (Oxford: Pergamon)
[2] London H 1940 *Proc. R. Soc.* A **176** 522
[3] Lieberman M A and Lichtenberg A J 1994 *Principles of Plasma Discharges and Materials Processing* (New York: Wiley)
[4] Lifshits I M, Azbel' M Ya and Kaganov M I 1973 *Electron Theory of Metals* (New York: Consultants Bureau)
[5] Kolobov V I and Economou D J 1996 *University of Houston Plasma Processing Laboratory Memorandum* PPL-063096
[6] Pippard A B 1947 *Proc. R. Soc.* A **191** 385
[7] Reuter G E H and Sondheimer E H 1948 *Proc. R. Soc.* A **195** 336
[8] Platzman P M and Wolff P A 1973 *Waves and Interactions in Solid State Plasmas* (New York: Academic)
[9] Demirkhanov R A, Kadysh I Ya and Khodyrev Yu S 1964 *Sov. Phys.–JETP* **19** 791
[10] Weibel E S 1967 *Phys. Fluids* **10** 741
[11] Kofoid M J 1969 *Phys. Fluids* **12** 1290
[12] Reynolds J A, Blevin H A and Thonemann P C 1969 *Phys. Rev. Lett.* **22** 762
[13] Blevin H A, Reynolds J A and Thonemann P C 1970 *Phys. Fluids* **13** 1259
[14] Blevin H A, Greene J M, Jolly D L and Storer R G 1973 *J. Plasma Phys.* **10** 337
[15] Storer R G and Meaney C 1973 *J. Plasma Phys.* **10** 349
[16] Storer R G 1973 *Phys. Fluids* **16** 949
[17] Blevin H A, Reinolds J A and Thonemann P C 1973 *Phys. Fluids* **16** 82
[18] Jolly D L 1976 *Sov. Phys.–JETP* **18** 337
[19] Joye B and Schneider H 1978 *Helv. Phys. Acta* **51** 804
[20] Sayasov Yu S 1979 *Helv. Phys. Acta* **52** 288
[21] Liberman M A, Meierovich B E and Pitaevskii L P 1972 *Sov. Phys.–JETP* **35** 904
[22] Dikman S M and Meierovich B E 1973 *Sov. Phys.–JETP* **37** 835
[23] Vasil'ev A N and Meierovich B E 1974 *Sov. Phys.–JETP* **40** 865
[24] Landau L D and Lifshitz E M 1984 *Electrodynamics of Continuous Media* (Oxford: Pergamon)
[25] Shkarofsky I P, Johnson T W and Bachinski M P 1966 *The Particle Kinetics of the Plasmas* (Reading, MA: Addison-Wesley)
[26] Lister G G, Li Y-M and Godyak V A 1996 *J. Appl. Phys.* **79** 8993
[27] Huba J D 1994 *NRL Plasma Formulary* (Washington, DC: Naval Research Laboratory)
[28] Okuno Y, Ohtsu Y and Fujita H 1994 *Appl. Phys. Lett.* **64** 1623
[29] Gantmakher V F 1967 *Prog. in Low-Temp. Phys.* **5** 181
[30] Eckert H U 1986 *Proc. 2nd Int. Conf. on Plasma Chemistry Technology (San Diego, 1984)* ed H V Boenig (Lancaster, PA: Technomic)
[31] Cohen R H and Rognlien T D 1996 *Phys. Plasmas* **3** 1839
[32] Gradshteyn I S and Ryzhik I M 1994 *Table of Integrals, Series, and Products* (San Diego, CA: Academic)
[33] Turner M M 1993 *Phys. Rev. Lett.* **71** 1844
[34] Meierovich B E 1970 *Sov. Phys.–JETP* **10** 782
[35] Meierovich B E 1971 *Sov. Phys.–JETP* **31** 149
[36] Hopwood J, Guarnieri C R, Whitehair S J and Cuomo J J 1993 *J. Vac. Sci. Technol.* A **11** 147
[37] Turner M M 1996 *Plasma Sources Sci. Technol.* **5** 159
[38] Vahedi V, Lieberman M A, DiPeso G, Rognlien T D and Hewett D 1995 *J. Appl. Phys.* **78** 1446
[39] Shaing K C 1996 *Phys. Plasmas* **3** 3300
[40] Godyak V A and Piejak R B 1996 unpublished
[41] Kaganovich I D, Kolobov V I and Tsendin L D 1996 *Appl. Phys. Lett.* **69** 3818
[42] Cohen R H and Rognlien T D 1996 *Plasma Sources Sci. Technol.* **5** 442
[43] Gibbons M R and Hewett D W 1995 *J. Comput. Phys.* **120** 231
[44] Kolobov V I, Lymberopoulos D P and Economou D J 1997 *Phys. Rev.* E **55** at press
[45] Tuszewski M 1996 *Phys. Rev. Lett.* **77** 1286
[46] Yoon N S, Kim S S, Chang C S and Choi Duk-In 1996 *Phys. Rev.* E **54** 757